nature immunology

Transcriptional insights into the CD8+ T cell response to infection and memory T cell formation

J Adam Best[1], David A Blair[2], Jamie Knell[1], Edward Yang[1], Viveka Mayya[2], Andrew Doedens[1], Michael L Dustin[2], Ananda W Goldrath[1] & The Immunological Genome Project Consortium[3]

After infection, many factors coordinate the population expansion and differentiation of CD8+ effector and memory T cells. Using data of unparalleled breadth from the Immunological Genome Project, we analyzed the CD8+ T cell transcriptome throughout infection to establish gene-expression signatures and identify putative transcriptional regulators. Notably, we found that the expression of key gene signatures can be used to predict the memory-precursor potential of CD8+ effector cells. Long-lived memory CD8+ cells ultimately expressed a small subset of genes shared by natural killer T and γδ T cells. Although distinct inflammatory milieu and T cell precursor frequencies influenced the differentiation of CD8+ effector and memory populations, core transcriptional signatures were regulated similarly, whether polyclonal or transgenic, and whether responding to bacterial or viral model pathogens. Our results provide insights into the transcriptional regulation that influence memory formation and CD8+ T cell immunity.

The Immunological Genome (ImmGen) Project is a partnership between immunologists and computational biologists with the goal of carefully and comprehensively defining gene-expression and regulatory networks in cells of the mouse immune system by highly standardized methods of sample collection and data preparation[1]. Here we sought to identify and track the transcriptional programs initiated in CD8+ T cells during the response to *in vivo* activation by bacterial or viral antigens. CD8+ cytotoxic T cells have important roles in the clearance of intracellular pathogens and tumors. In the uninfected state, a diverse repertoire of resting, naive CD8+ T cells populate peripheral lymphoid organs. After infection, CD8+ T cells transition from quiescent, poor effector cells to metabolically active, proliferating cells with cytolytic function and the capacity for rapid cytokine production. That progression is accompanied by changes in gene expression that reflect each stage of differentiation[2–5]. During expansion, the innate immune response induced by different pathogens creates infection-specific inflammatory environments that influence the kinetics of T cell population expansion and the effector differentiation and memory potential of CD8+ T cells[6,7]. However, the effect of such unique proinflammatory environments on transcriptional networks and gene expression by CD8+ T cells is not well understood.

After pathogen clearance, most CD8+ T cells die, which leaves a select few with the ability to form long-term memory and to protect the host from reinfection. Each differentiation state—naive, effector, terminally differentiated effector and memory—is thought to be orchestrated by a network of transcription factors with key downstream targets that enable and enforce stage-specific cellular traits. In confirmation of that, certain transcriptional activators or repressors are well established as essential regulators of gene expression by CD8+ T cells during infection, including those encoded by *Tbx21*, *Tcf7*, *Eomes*, *Id2*, *Id3* and *Prdm1*, yet it is likely that many additional factors that affect CD8+ T cell differentiation are yet to be described. Such factors are more efficiently identified by unbiased methods such as transcriptomics.

CD8+ T cells are known to share certain functional abilities and transcription factors with other cells of the immune system; however, the transcriptional relationship between CD8+ T cells and other cytolytic lymphocyte populations is not well described. The ImmGen Program offered a unique opportunity to address this question, given its unmatched inventory of directly comparable transcriptomic data for hundreds of different types of cells of the immune system. We have made a systematic and temporally resolved analysis of transcriptional changes that occur through the antigen-specific responses of CD8+ T cells, from early time points of activation to the analysis of long-term memory cells, in the context of various infection settings. From these data, we have identified previously unknown clusters of coregulated genes and used network-reconstruction analyses of the ImmGen Consortium to predict transcriptional activators and repressors or genes with differences in expression. These analyses allowed us to profile CD8+ T cells with differing memory potential and obtain insights into the transcriptional processes that govern the differentiation of effector and memory cell populations.

RESULTS

Temporally regulated expression patterns in CD8+ T cells

To establish a molecular profile of pathogen-reactive CD8+ T cells over the course of infection, we transferred congenic naive OT-I T

[1]Division of Biological Sciences, University of California San Diego, La Jolla, California, USA. [2]Skirball Institute of Biomolecular Medicine, New York University School of Medicine, New York, New York, USA. [3]A list of members and affiliations appears at the end of the paper. Correspondence should be addressed to A.W.G. (agoldrath@ucsd.edu).

Received 9 August 2012; accepted 21 December 2012; published online 10 February 2013; doi:10.1038/ni.2536

cells (which have transgenic expression of a T cell antigen receptor (TCR) that recognizes a fragment of ovalbumin (OVA; amino acids 257–264) presented by the major histocompatibility complex molecule H-2K^b) into C57BL/6J mice, which we then immunized with OVA-expressing *Listeria monocytogenes* (Lm-OVA) as a model pathogen-associated antigen. We collected splenic CD8$^+$ T cells on days 6, 8, 10, 15, 45 and 100 of infection and sorted the cells to high purity for gene-expression profiling by the ImmGen data-generation and quality-control pipelines (**Supplementary Fig. 1a** and **Supplementary Note 1**). We transferred the minimum number of OT-I cells that still allowed adequate recovery of responding cells for analysis. For collection on days 6 and later, we transferred 5×10^3 donor cells 1 d before immunization, which represented a relatively low precursor frequency, albeit higher than the endogenous repertoire of T cells specific for H2-K^b–OVA peptide[8,9]. To gain better understanding of the changes in gene expression that occur during the earliest stages of the response after activation, before the expansion phase, we used the following alternative approach: we first infected mice with Lm-OVA and, 1 d later, transferred OT-I CD8$^+$ cells into the mice and then isolated the cells on days 0.5, 1 and 2 after transfer. This approach included a greater frequency of precursor cells (1×10^6 transferred cells) and allowed the infection to become established so that transferred OT-I cells were rapidly recruited into the immune response. The expression of markers associated with activation and differentiation by these cells was similar to that of cells transferred at a lower precursor frequency (5×10^3 transferred cells), and any differences were consistent with more rapid contraction and differentiation into the memory subset (**Supplementary Fig. 2**). We analyzed the transferred OT-I CD8$^+$ T cells by flow cytometry for expression of phenotypic markers of activation and/or memory. We found that expression CD127, CD62L and CD27 was downregulated with activation, followed by reexpression in memory cells, whereas the expression of CD69 and CD44 was uniformly upregulated, as expected (**Supplementary Fig. 1b**), which indicated that all of the transferred cells were activated.

The number of genes with different expression in infection-exposed OT-I cells versus naive OT-I cells peaked within 48 h of infection; unexpectedly, at later time points, a greater proportion of genes with altered expression were downregulated than were upregulated (**Fig. 1a**),

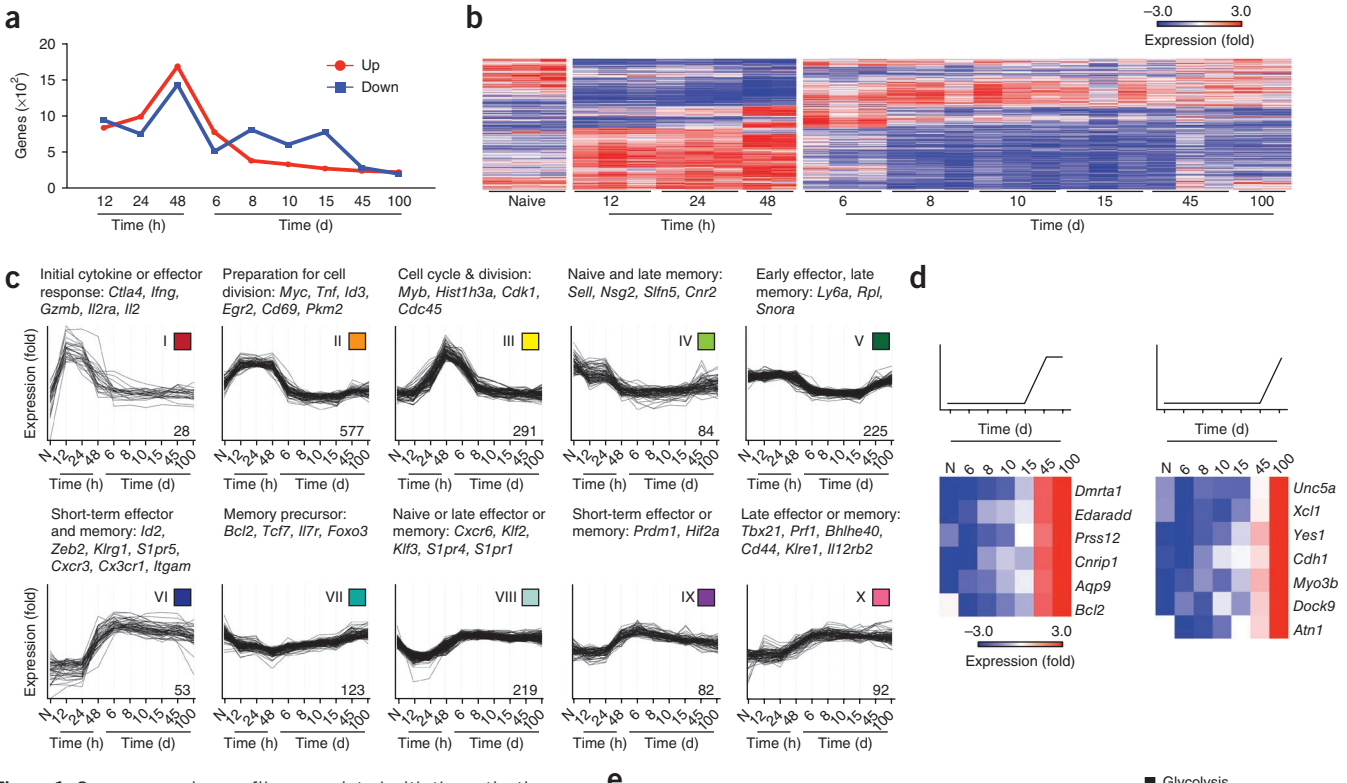

Figure 1 Gene-expression profiles associated with the activation and memory formation of CD8$^+$ T cells. (**a**) Quantification of genes upregulated (Up) or downregulated (Down) in infection-exposed OT-I cells relative to their expression in naive OT-I cells at various time points during infection (horizontal axis). (**b**) Hierarchical clustering analysis of OT-I cells sorted at various time points after infection with Lm-OVA, filtered for a change in expression of over twofold anywhere in the data set, a coefficient of variation of less than 0.5 and mean expression value of over 120. (**c**) Ten clusters with the most dynamic expression by *K*-means clustering analysis, filtered as in **b** but with a change in expression of over 1.4-fold. Each line represents a single probe; numbers in bottom right corners indicate number of probes; above plots, genes of interest in each cluster. (**d**) Heat map (bottom) of the correlation coefficients of mean gene expression fit to an artificial exemplar (top) of genes upregulated only at day 45 and day 100 of infection (left) or of genes upregulated only at day 100 (right), showing the top 15% of correlated genes. (**e**) Quantification of genes in each cluster a given gene ontology (GO) tag related to metabolism (key), presented relative to all genes with that tag. Data are representative of three experiments with a compilation of two (48 h and day 100) or three (all other time points) independent samples sorted from pooled spleens ($n \geq 3$ per sample).

which suggested that the transition to memory required a tempering of gene expression associated with initial activation. To visualize changes in gene expression over the course of the CD8$^+$ T cell response to infection with Lm-OVA, we selected 7,195 genes that had a difference in expression of at least twofold in any two samples in the data set from the total of 25,194 genes examined (**Fig. 1b** and **Supplementary Table 1**). We next parsed those probes with differences in expression into unbiased groups according to kinetic patterns of expression (by *K*-means clustering). We further investigated the ten clusters with the most dynamic patterns.

To determine the biological processes probably associated with each cluster, we identified groups of genes that shared gene-ontology designations (**Fig. 1c** and **Supplementary Table 2**). Cluster I included genes with expression that was upregulated 12 h after activation, then decreased immediately but remained higher than that in naive cells. This cluster had the fewest genes and notably included genes encoding early effector molecules. Cluster II had the most genes (577); a large proportion encoded RNA-processing molecules or molecules related to RNA processing, but this cluster also included genes downstream of TCR activation, such as *Egr2* and *Cd69*. As expected, genes in cluster III encoded molecules mostly related to the cell cycle and proliferation, processes coincident with the proliferative burst. Cluster IV included genes with the highest expression in naive and memory CD8$^+$ T cells, such as *Sell* (which encodes CD62L), and genes encoding molecules suspected to have roles in suppressing the immune response, including *Cnr2* and *Slfn5*. The genes of cluster V mostly encoded ribosomal proteins and small nuclear RNAs and had moderate expression in naive and early activated cells as well as in the memory population. Cluster VI included genes that encode phenotypic markers traditionally associated with effector and effector-memory CD8$^+$ subsets, such as KLRG1, CD11b and Id2, as well as migratory receptors, such as S1PR5 and CX3CR1. Genes associated with memory-precursor cells were present in cluster VII, including *Il7r*, *Bcl2* and *Tcf7*. Gene expression in cluster VIII was lower in cells responding to infection than in naive T cells early in the response, and expression recovered after day 6; gene expression in cluster IX was low in naive cells, then rose and then fell slowly over time; whereas gene expression in cluster X remained high into memory time points.

Included in clusters IX and X were many genes whose products have known roles in memory formation, such as T-bet (*Tbx21*) and Blimp-1 (*Prdm1*), in addition to inflammatory receptors such as S1PR1 and the interleukin 12 receptor (IL-12R), and Krüppel-like-factors, which have been linked to proliferation and survival[10]; this provided early confirmation of the validity of the technique. More unexpected was the rapid upregulation of expression of effector molecules such as granzyme B, interferon-γ and IL-2, encoded by genes of cluster I. Although it has been shown in reporter mice that an interferon-γ signal can be detected as early as 24 h after immunization with OVA peptide–pulsed dendritic cells[11], our data suggested that the gain of effector function that occurred with priming was initiated as early as 12 h after antigen recognition.

To identify unique genes encoding molecules potentially involved specifically in the function of memory and late memory CD8$^+$ T cells, we looked for transcripts that correlated with an exemplar of each cluster (genes not expressed until day 45 or day 100; $R^2 > 0.85$). Very few genes met those strict criteria; we identified six genes as 'memory specific' and seven as 'late-memory specific'. We confirmed mRNA abundance by quantitative PCR (**Fig. 1d** and **Supplementary Fig. 3**). According to those criteria, no genes were specifically downregulated at the later time points, which was unexpected, given the quiescent state of memory cells. As anticipated, *Bcl2* expression was higher in the memory subset; *Bcl2* expression has been linked to memory formation and survival, consistent with the emergence of long-lived memory cells from the heterogeneous pool of effector-memory populations[12]. That observation enhanced our confidence in the accuracy of our identification of memory-specific and late-memory-specific genes, never before associated with memory formation and/or maintenance, to our knowledge. Notably, we identified *Cdh1* as a late-memory-specific gene. Its product, E-cadherin, is a calcium-dependent homophilic adhesion molecule and a ligand of the effector-cell marker KLRG1 (ref. 13) and the integrin CD103 (ref. 14). This suggested that the oldest memory cells may be capable of unique adhesive interactions and may access distinct microenvironmental niches. Expression may also serve as a unique surface identifier of late-memory cells.

As the metabolic regulation of the differentiation of memory T cells is a topic of broad interest, we used gene-ontology annotations to examine the expression of genes encoding molecules in specific metabolic pathways. Genes encoding glycolysis-related molecules were almost exclusively in cluster II, whereas genes encoding molecules related to the respiratory chain and fatty-acid metabolism were distributed among clusters II, III, V and VIII; the former two clusters represented rapidly dividing cells and included genes encoding molecules involved in fatty-acid biosynthesis, whereas the latter two clusters included genes maintained in naive cells as well as memory cells and those encoding molecules involved in the transport of acetyl-CoA and fatty-acid oxidation (**Fig. 1e** and **Supplementary Table 2**). These data supported the observation that a switch from glycolysis to fatty-acid metabolism is necessary for proper memory formation[15–17].

Predicted regulators of the T cell response

The breadth of information in the data set from the ImmGen Project provided a platform with which to investigate the basis of the different patterns of gene regulation observed across the ten clusters of CD8$^+$ T cells identified. As part of the global analysis of the ImmGen Project, which includes all types of cells of the immune system, we used cutting-edge network reverse engineering to identify potential regulators of gene expression[18] (metadata, http://www.immgen.org/ModsRegs/modules.html). Each 'module' of the ImmGen Project consists of groups of coregulated genes identified from the entire data set of the ImmGen Project (explanation of modules, ref. 18; modules, http://www.immgen.org/ModsRegs/modules.html). We then used the Ontogenet algorithm[18] to predict likely transcriptional regulators for each module on the basis of the expression profile of those gene sets, 'leveraged' by analysis including all data from the ImmGen Project. To determine where our activated CD8$^+$ T cell clusters were in those modules, we used a hypergeometric test for two groups (comparing each CD8$^+$ T cell cluster to each fine module) to identify any statistically significant enrichment for genes of clusters I–X in fine modules of the ImmGen Project (with application of a Benjamini-Hochberg false-discovery rate of 0.05 or lower to the *P*-value table of all ten clusters throughout all fine modules). We found that several fine modules showed significant enrichment for genes of each cluster (**Supplementary Fig. 4a** and **Supplementary Table 3**). For example, fine module 99, which includes genes expressed in natural killer (NK) cells, NKT cells and activated CD8$^+$ T cells, showed the most significant enrichment for genes in cluster X. Associated with each fine module were predicted transcriptional 'regulators' of the genes identified in each cluster, each with a 'regulatory weight' in a given cell type that indicates its activity as a regulator for a particular module in a particular cell type. We pooled predicted activators or repressors from all of the fine modules that showed enrichment

Figure 2 Coregulated genes can be used to predict transcriptional regulation of T cell activation. Enrichment for genes in activated CD8+ T cell clusters (identified in **Fig. 1**) in the context of fine modules of coregulated genes identified by the ImmGen Consortium, for genes encoding selected regulators of T cells (key) predicted through the use of the Ontogenet algorithm[18] based on enriched modules (**Supplementary Fig. 4**), 'curated' by relevance to T cell biology and in order of predicted weight, for which genes with a 'weight' of 0 do not contribute to the regulatory program of that cell population.

T cells
$CD8^+$ T cells
Activated $CD8^+$ T cells

	Predicted activators	Predicted repressors
I	*Tbx21*, *Id2*, *Relb*, *Rora*, *Klf12*, *Smyd1*, *Eomes*, *Nab1*, *Stat4*, *Runx2* (regulator weights: 0.199 to 0.00468)	*Pou2af1*, *Pax5*, *Mycn*, *Ebf*, *Pparg*, *Cebpb* (regulator weights: –0.00086 to –0.0215)
II	*Churc1*, *Phf5a*, *Cbx5*, *Hdac6*, *Taf9*, *Mybl2*, *E2f1*, *Elof1*, *E2f6*, *Nkrf*, *Myc*, *Tfdp2* (regulator weights 0.131 to 0.0743)	*Insm1*, *Scmh1*, *Klf3*, *Runx1*, *Cited2*, *Foxd4*, *Nfkbia*, *Foxp1*, *Arntl*, *Tcf7*, *Foxj2* (regulator weights: –0.00032 to –0.0493)
III	*Uhrf1*, *Dnmt1*, *Foxm1*, *E2f8*, *Suv39h1*, *Hmgb2*, *Tcf19*, *E2f7*, *Hat1*, *Whsc1* (regulator weights: 0.0130 to 0.00794)	*Klf12*, *Ciita*, *Nfe2l1*, *Chd7*, *Foxj2* (regulator weights: –0.00006 to –0.0807)
IV	*Ets1*, *Irf7*, *Irf9*, *Bcl11b*, *Elk4*, *Lef1*, *Tox*, *Trim14*, *Tcf7*, *Gata3*, *Nfatc3*, *Nfatc1*, *Egr2*, *Nab2*, *Foxo1*, *Zbtb7b*, *Stat2*, *Tcfe3*, *Irf1*, *Ets2*, *Hif1a* (regulator weights: 0.129 to 0.0101)	*Runx2*, *Mybl1*, *Klf12*, *Lmo2*, *Egr3*, *Scmh1*, *Rorc*, *Smad3*, *Irf8*, *Notch3*, *Tbx21*, *Tcfe2a*, *Stat6*, *Ctbp2*, *Cux1*, *Tcf4*, *Irf5* (regulator weights: –0.00007 to –0.0735)
V	*Cnbp*, *Smyd3*, *Myc*, *Elof1*, *Hat1*, *Zeb1*, *Rarb*, *Hdac2*, *Atoh1*, *Smad7*, *Stat2* (regulator weights: 0.135 to 0.00058)	*Foxd4*, *Tbx6*, *Mycl1*, *Ppard*, *Cited2*, *Cbx2*, *E2f4* , *Klf7*, *Runx3*, *Pbrm1* (regulator weights: –0.00011 to –0.0188)
VI	*Nab1*, *Klf6*, *Irf5*, *Tcfe3*, *Rxra*, *Id2*, *Ciita*, *Pias3*, *Eomes*, *Rara*, *Klf12*, *Relb*, *Rora*, *Smyd1*, *Runx2*, *Smad3*, *Stat4*, *Prdm1*, *Zeb2* (regulator weights: 0.117 to 0.00182)	*Taf2*, *Pax5*, *Hic1*, *Mycn*, *Nfkb1*, *Pparg*, *Relb*, *Cebpb*, *Zfhx3*, *Ebf1*, *Maf*, *Gata3*, *Mllt3*, *Bcl11b* (regulator weights: –0.00039 to –0.0826)
VII	*Tbx21*, *Gata3*, *Nfatc3*, *Lef1*, *Tox*, *Nfatc1*, *Bcl11b*, *Tcf7*, *Pias1*, *Foxo3*, *Tcf4* (regulator weights: 0.0953 to 0.00294)	*Prmt5*, *Chd7*, *Nfix*, *Klf3*, *E2f2*, *Tcf4*, *Irf5*, *Mef2c*, *Lmo2* (regulator weights: –0.00077 to –0.10023)
VIII	*Nfatc2*, *Nab1*, *Stat6*, *Ets1*, *Bcl11b*, *Irf7*, *Lef1*, *Gata3*, *Tcfe3*, *Klf6*, *Smad7*, *Tcf7*, *Tox*, *Id2*, *Rxra*, *Foxo4*, *Foxo3*, *Tbx21*, *Smad4*, *Eomes* (regulator weights: 0.199 to 0.0262)	*Stat2*, *Tcf20*, *Nfkb1*, *Nfatc1*, *Relb*, *Creg1*, *Tcf4*, *Insm1*, *Zeb1*, *Tcfeb*, *Klf8*, *Tcfe2a*, *Pax5*, *Bcl6*, *Foxp4*, *Ctbp2* (regulator weights: –0.00042 to –0.0231)
IX	*Rxra*, *Tcfe3*, *Stat6*, *Irf5*, *Id2*, *Smad2*, *Klf6*, *Tbx21*, *Eomes*, *Smad3*, *Prdm1* (regulator weights: 0.0758 to 0.00097)	*Maf*, *Scmh1*, *Zbtb7b*, *Pax5*, *Zeb1*, *Hmgn3*, *Satb1*, *Foxp4*, *Hdac7*, *Ets1* (regulator weights: –0.00028 to –0.0641)
X	*Tbx21*, *Nab1*, *Tcfe3*, *Irf5*, *Id2*, *Runx2*, *Foxp1*, *Eomes*, *Rora*, *Smyd1*, *Bhlhe41*, *Stat4*, *Zeb2*, *Runx3* (regulator weights: 0.199 to 0.00044)	*Maf*, *Etv3*, *Hic1*, *Mycn*, *Runx1*, *Pax5*, *Nab2*, *Prdm1*, *Srebf2*, *Pax5*, *Hdac7* (regulator weights: –0.00028 to –0.0854)

for genes from $CD8^+$ T cell clusters (I–X) and ranked them in order of the predicted regulatory weight. We used a linear model to generate a prediction of the expression of the modules' genes in each cell type on the basis of the activity-weighted expression of the regulators[18]. We assigned colors on the basis of their predicted role as regulators of gene expression (as indicated by the meta-analysis at http://www.immgen.org/ModsRegs/modules.html) in T cells, $CD8^+$ T cells or activated T cells (**Fig. 2**). We identified many genes encoding transcriptional regulators known to have roles in $CD8^+$ T cell activation and differentiation, including *Tbx21*, *Erg2*, *Egr3*, *Prdm1*, *Bcl11b*, *Tcf7*, *Bcl6*, *Foxo1*, *Foxo3*, *Id2*, *Tcf3* and many genes encoding STAT proteins (**Fig. 2** and **Supplementary Fig. 4**). For example, on the basis of these results, we predicted that the products of *Id2*, *Tbx21* and *Prdm1* in various combinations would positively regulate genes in clusters VI, IX and X, which include genes expressed in short-term effector-memory cells; it is known that the loss of each of these regulators results in impaired generation of this subset[19,20]. Conversely, we identified the *Tcf7* as encoding a regulator of the genes in clusters IV, VII and VIII, which include many genes associated with naive and long-term memory populations; it is known that loss of *Tcf7* impairs memory formation. Thus, this strategy holds promise for the identification of additional regulators of the $CD8^+$ T cell response.

The expression patterns of CD127 (IL-7R) and KLRG1 can be used to predict T cell fate early in the immune response[21–23]. IL-$7R^{lo}$KLRG1^{hi} cells have been identified as short-lived effector cells, whereas IL-$7R^{hi}$KLRG1^{lo} $CD8^+$ T cell populations include a subset of cells that go on to become long-lived memory cells and have been called 'memory-precursor effector cells'[19]. To put our data in context of that paradigm, we used published microarray data comparing the gene expression of IL-$7R^{hi}$ and IL-$7R^{lo}$ $CD8^+$ effector cells responding to infection with lymphocytic choriomenengitis virus[19] and analyzed the expression of those genes in the context of infection with Lm-OVA (**Supplementary Fig. 5**). Cells near the peak of infection showed enrichment for the majority (86%) of genes with higher expression in the IL-$7R^{lo}$ $CD8^+$ T cell population than in the IL-$7R^{hi}$ $CD8^+$ T cell population; these included genes encoding molecules involved in cell cycle and mitosis, almost half of which were in cluster III (**Supplementary Fig. 5a**,**c**). The IL-$7R^{lo}$ effector cell population showed enrichment for genes from clusters VI, IX and X; these included genes whose expression increased at the peak of infection (48 h) and then was sustained or decreased slowly in the memory phase (**Supplementary Fig. 5a**,**c**). Genes expressed by IL-$7R^{hi}$ cells near the peak of the response were upregulated only very late during infection when we evaluated expression by the $CD8^+$ population as a whole, which supported the idea that these cells truly represented precursors that seeded the long-term memory compartment (**Supplementary Fig. 5b**,**d**). Many of these genes 'turned off' by 48 h, not to re-emerge until day 45 of the response, which suggested that some priming of gene expression may have occurred very soon after antigen exposure.

We also identified many regulators whose involvement was previously unappreciated in the differentiation of $CD8^+$ T cell response by this strategy. Confirming a potential for predicted involvement, quantitative PCR showed that the abundance of *Rora*, *Zeb2*, *Tox*, *Ets1* and *Tcf19* mRNA was greater in the KLRG1^{hi} $CD8^+$ effector T cell subset than in KLRG1^{lo} effector cells sorted from the same response (**Supplementary Fig. 4c**). Comparison of the expression of those regulators in the context of KLRG1 expression provided preliminary information about their potential functions; for example, *Rora* and *Zeb2* were expressed 'preferentially' in the KLRG1^{hi} subset and both encode predicted positive regulators of genes in clusters VI and X, which include genes expressed by short-term effector, short-term memory and late effector-memory cells. These data suggested that the products of *Rora* and *Zeb2* and other previously unknown regulators may control the gene-expression patterns of those subsets of $CD8^+$ effector cells.

Core gene clusters during $CD8^+$ T cell differentiation

We next used the $CD8^+$ T cell cluster gene signatures identified above (**Fig. 1**) to correlate changes in gene expression during differentiation into short-lived effector-memory or long-term memory precursor cells. Inhibition of transcription factors of the E-protein family by Id2 and Id3 has been shown to alter $CD8^+$ T cell differentiation[24–26]. For example, loss of Id2 expression impairs the survival of effector cells and results in the failure to accumulate KLRG1^{hi} short-lived effector cells[24]. Conversely, Id3 is needed to sustain the long-lived memory population, and abundant Id3 expression can be used to predict memory-precursor potential[24]. To determine how differences in gene expression early in the immune response could be used to predict and were correlated with known memory potential of particular populations, we evaluated gene-expression profiles in the context of our ten expression clusters for three comparisons of $CD8^+$ effector populations: Id2-deficient versus Id2-wild-type KLRG1^{lo} OT-I cells from day 6 of infection; KLRG1^{lo}IL-$7R^{hi}$ versus KLRG1^{hi}IL-$7R^{lo}$ OT-I cells from day 6 of infection; and $Id3^{hi}$ versus $Id3^{lo}$ KLRG1^{lo}IL-$7R^{lo}$

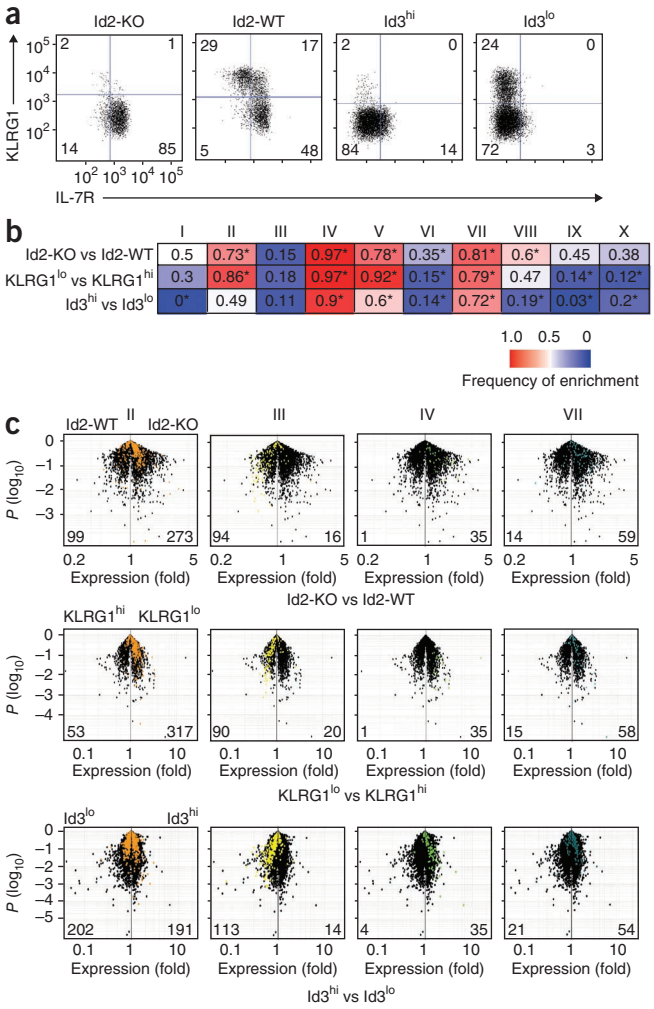

Figure 3 Regulation of core gene-expression modules by memory precursor cells. (**a**) Flow cytometry of CD8$^+$ T cells from Id2-deficient mice (Id2-KO) and Id2-wild-type mice (Id2-WT) and Id3^{hi} and Id3^{lo} CD8$^+$ T cells, on day 6 of infection with VSV-OVA. Numbers in quadrants indicate percent cells in each. (**b**) Heat map of the frequency of enrichment of clusters (**Fig. 1c**) in wild-type and Id2-deficient samples collected on day 6 of infection with Lm-OVA and Id3^{hi} and Id3^{lo} samples collected on day 5 of infection with VSV-OVA (both pre-peak time points) for the following comparisons: Id2-deficient versus wild-type cells (both KLRG1^{lo}IL-7R^{hi}; top), KLRG1^{lo}IL-7R^{hi} cells versus KLRG1^{hi}IL-7R^{lo} cells (both wild-type; middle), or Id3^{hi} versus Id3^{lo} cells (both CD44$^+$KLRG1^{lo}IL-7R^{lo}; bottom). Numbers in map indicate proportion of cells with enrichment for that comparison; a frequency of 1.0 (red) indicates memory potential, and a frequency of 0.0 (blue) indicates effector potential. $^*P < 0.05$ (χ^2 test). (**c**) 'Volcano plots' of the comparison of Id2-deficient KLRG1^{lo} cells versus wild-type KLRG1^{lo} cells (top), wild-type KLRG1^{lo} cells versus wild-type KLRG1^{hi} cells (middle), and Id3^{hi} cells versus Id3^{lo} cells (bottom), showing cluster-specific genes for each comparison. Numbers in bottom right and left corners indicate the number of genes in that region. Data are representative of three independent experiments with three mice per genotype (**a**) or three experiments with three independent samples from pooled spleens (**b**,**c**; $n \geq 3$ per sample).

OT-I cells, sorted on the basis of their expression of a green fluorescent protein (GFP) reporter of Id3 on day 5 of infection[24] (**Fig. 3a**). In each comparison, cells with greater memory potential were in the first population listed. We assessed whether genes from each cluster were biased toward cells with memory potential versus effector potential in any of the comparisons (**Fig. 3b**); here, we determined 'enrichment' by the fraction of genes with a change in expression of over onefold (versus the null hypothesis of independence of 0.5). This analysis shows skewing for many of the key CD8$^+$ T cell gene clusters: genes in clusters III, VI, IX and X, which included many of the effector and effector-memory associated genes, were 'preferentially' expressed in the Id2-wild-type, KLRG1^{hi} and Id3^{lo} populations, whereas genes in clusters IV, V and VII, which included genes associated with naive, early effector and late memory, were 'preferentially' expressed in the Id2-deficient, KLRG1^{lo} and Id3^{hi} populations.

To further demonstrate the relative gene expression in the three comparisons, we generated plots of each comparison for clusters II, III, IV and VII (**Fig. 3c**). We found considerable enrichment for genes linked to cluster IV (naive and late memory) and cluster VII (memory precursor) in Id2-deficient, KLRG1^{lo} and Id3^{hi} cells (**Fig. 3b**); 90–97% of the genes in cluster IV and 72–81% of those in cluster VII had higher expression in Id2-deficient, KLRG1^{lo} and Id3^{hi} cells than their counterpart populations (Id2-wild-type, KLRG1^{hi} and Id3^{lo}, respectively). This analysis also provided several unexpected observations. Of particular interest to us was cluster II, for which genes encoding molecules associated with proliferation and division were expressed differently by Id2-deficient versus Id2-wild-type cells and by KLRG1^{hi} cells versus KLRG1^{lo} cells but had equivalent expression in Id3^{hi} cells and Id3^{lo} cells. Notably, all three comparisons indicated that the subset of cells biased toward memory precursor potential had lower expression of genes in cluster III (cell cycle and division) and cluster IV (short-term effector memory) than did their more short-lived effector counterparts, even at the peak of expansion (**Fig. 3a**,**c**). These data suggested that the earliest phases of the immune responses in the context of deficiency in Id2 or Id3 may have previously unappreciated differences in activation or division based on the temporal regulation of genes in cluster II and III, defects not identified in earlier analyses of deficient cells. Furthermore, although it has been reported to be homogeneous, the population assumed to contain memory precursors may actually be more heterogeneous than previously thought.

TCR clonality does not alter core gene signatures

Many immunological advances have made use of model pathogens and donor cells with transgenic expression of TCRs that can be monitored by artificially high precursor frequency and/or expression of congenic markers. However, it is known that the broader range of affinity and lower precursor frequency of polyclonal endogenous CD8$^+$ T cell responses, as well as pathogen-specific inflammatory environments, lead to differences in the differentiation of effector and memory cells, including the induction of T-bet expression during infection with *L. monocytogenes*[27–29]. We therefore sought to determine if differences in TCR repertoire and frequency led to changes in the expression of core gene clusters. We used tetramers of H-2K^b loaded with OVA peptide to identify endogenous, antigen-specific CD8$^+$ T cells from nontransgenic mice infected with Lm-OVA on days 8 and 45 of infection (**Supplementary Fig. 6**). We used the resultant profiling data to compare the transcriptional response of polyclonal OVA peptide–specific (tetramer-positive) cells with that of OT-I T cells, across the gene clusters identified above (**Fig. 1**). Few genes had a difference in expression of over twofold in transgenic cells versus tetramer-positive OVA peptide–specific cells at day 8, and even fewer had such a difference in expression at day 45 of infection (**Fig. 4a**), which suggested that the frequency of antigen-specific T cell precursors and TCR repertoire did not greatly alter gene expression at effector or memory time points. The few genes found to be

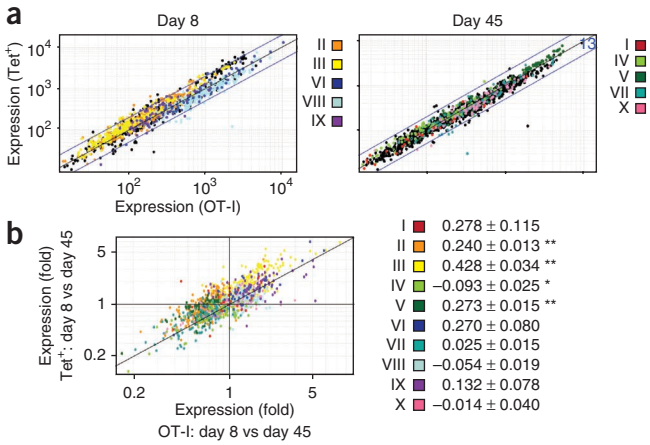

Figure 4 Common gene-expression patterns of transgenic and endogenous CD8+ effector and memory T cells. (**a**) Difference in gene expression of H-2K^b–OVA tetramer–positive antigen-specific (endogenous) cells (Tet+) versus OT-I cells (OT-I) on day 8 or day 45 of infection with Lm-OVA, for genes identified by *K*-means clustering analysis (**Fig. 1**); colors in plots (genes) match colors of clusters (key); blue diagonal lines indicate a difference in expression of twofold. (**b**) Comparison of gene expression on day 8 versus day 45 after infection as in **a** for tetramer-positive cells, plotted against that for OT-I CD8+ T cells; colors in plots (genes) match colors of clusters (key); values in key indicate the change in expression (mean $y_i - x_i$) ± s.e.m.; diagonal line indicates $y = x$. $^*P < 0.001$ and $^{**}P < 0.00001$ (*t*-test). Data are representative of two independent experiments with three mice per group.

regulated differently in the two cell types were almost exclusively genes encoding TCRs, ribosomal proteins and small nuclear RNAs. The only notable exceptions were modest enrichment for *Klra3*, *Klra8 and Klra9* transcripts in OT-I cells (data not shown); *Klra3*, *Klra8 and Klra9* had 1.9-, 1.8- and 2.4-fold higher expression, respectively, in tetramer-positive cells than in naive cells and had 3.3-, 2.4- and 3.9-fold higher expression, respectively, in OT-I cells than in naive cells. By comparing the ratio of expression at day 8 to that at day 45 for OT-I and tetramer-positive cells, we observed a similar 'evolution' of gene expression in both conditions, but it was also apparent that genes in clusters II and III had a small but uniformly higher ratio of expression by polyclonal tetramer-positive effector and memory populations (**Fig. 4b**). As clusters II and III included many genes encoding molecules involved in cell cycle and division, this suggested that the priming event for a low-frequency, antigen-specific T cell population drove more proliferation of those cells, perhaps because of less competition for antigen and activation signals than the competition encountered by high-frequency precursor cells, for which such signals may be limiting. Notably, however, examination of clusters linked to memory potential or formation (clusters VI–X) showed that most genes were regulated similarly in the two populations. Thus, by genome-wide assessment of gene expression, our data showed that endogenous and monoclonal responses reflected similar 'transcriptional programming' during memory formation and supported the conclusion that the small number of phenotypic differences used to suggest differences in memory formation in this context[8,30] do not represent a substantial divergence in core gene signatures.

Similar gene signatures during different infections

The immune response tailors itself to each pathogenic threat by responding to molecular cues, including the inflammatory cytokine milieu, antigen load, innate signaling and requirements for CD4+ T cell help, all of which can affect the number of T cells recruited to the response, the kinetics of their activation, and their differentiation fate as effector and memory cells. We sought to determine if there were notable differences in the transcriptional response to stimulation by the same antigen in the context of a bacterial infection versus a viral infection. To contrast with the Lm-OVA model analyzed above, we used vesicular stomatitis virus expressing recombinant ovalbumin (VSV-OVA). We transferred OT-I cells as described above and subsequently infected the recipient mice with either agent. We then collected OT-I cell–derived CD8+ T cells and profiled them as described above.

When we plotted the overall responses, it was apparent that expression patterns over each time course were generally similar, with sequential induction and 'shut-off' of the same blocks of genes (**Fig. 5a**). Some distinctions were detectable; for example, a group of transcripts repressed during the effector period were not reinduced as effectively after infection with VSV-OVA as after infection with Lm-OVA. The induction and contraction of the response after infection with VSV-OVA or Lm-OVA were generally superimposable for the same core gene signatures identified by clusters I–X (**Fig. 5b**), which suggested that many aspects of the CD8+ T cell responses were antigen focused and 'blind' to pathogen-specific inflammatory events.

To better delineate differences between the responses, we used analysis of variance (ANOVA); for simplicity, we grouped the results obtained for days 5–10 and days 45–100 into the effector phase and memory phase, respectively. We identified a few distinct transcripts (with a change in expression of over twofold) by this analysis (**Fig. 5c** and **Supplementary Table 4**). For example, *Klrg1* was induced more effectively during infection with Lm-OVA, whereas *Ctla4* and *Pdcd1* (which encodes the costimulatory molecule PD1) had higher expression during infection with VSV-OVA; these differences tended to be conserved at the effector and memory phases (**Fig. 5c**). We confirmed several of those differences at the protein level by flow cytometry; the results reflected expression differences by a subset of cells (CTLA-4 and KLRG1) and different expression by the population as a whole (PD-1; **Fig. 5d**). Genes known to be IL-12 dependent[31] during infection had moderately higher expression during infection with Lm-OVA (**Supplementary Fig. 7a**). However, this was mainly a difference in magnitude, in that most of the IL-12-responsive genes were upregulated in both infections but were upregulated to a greater extent after infection with Lm-OVA than after infection with VSV-OVA (**Supplementary Fig. 7b**). We found a very similar pattern for genes responsive to type I interferons[31], with moderate skewing toward infection with Lm-OVA (**Supplementary Fig. 7c**); however, again this was largely due to subtle differences in magnitude (**Supplementary Fig. 7d**). These data may yield insight into the more rapid contraction of T cell populations responding to VSV than of those responding to *L. monocytogenes*. However, whereas the differences after infection with Lm-OVA or with VSV-OVA were quantitative, there was minimal indication of transcripts uniquely affected in one condition or the other (**Supplementary Table 4**). Despite the distinct milieu elicited by bacterial and viral infection, the core gene-expression programs of our ten clusters were conserved in the CD8+ effector and memory populations (**Fig. 5e**), and the few differences tended to represent differences in the amplitude of expression.

Shared signatures of functionally related cell types

Many cell types of the immune system share conserved gene-expression modules. Using data from the ImmGen Project, we compared pairs of B cell, NKT cell and γδ T cell populations to identify any statistically significant enrichment for genes from our CD8+ T cell clusters during their activation, as a clue to differentiation

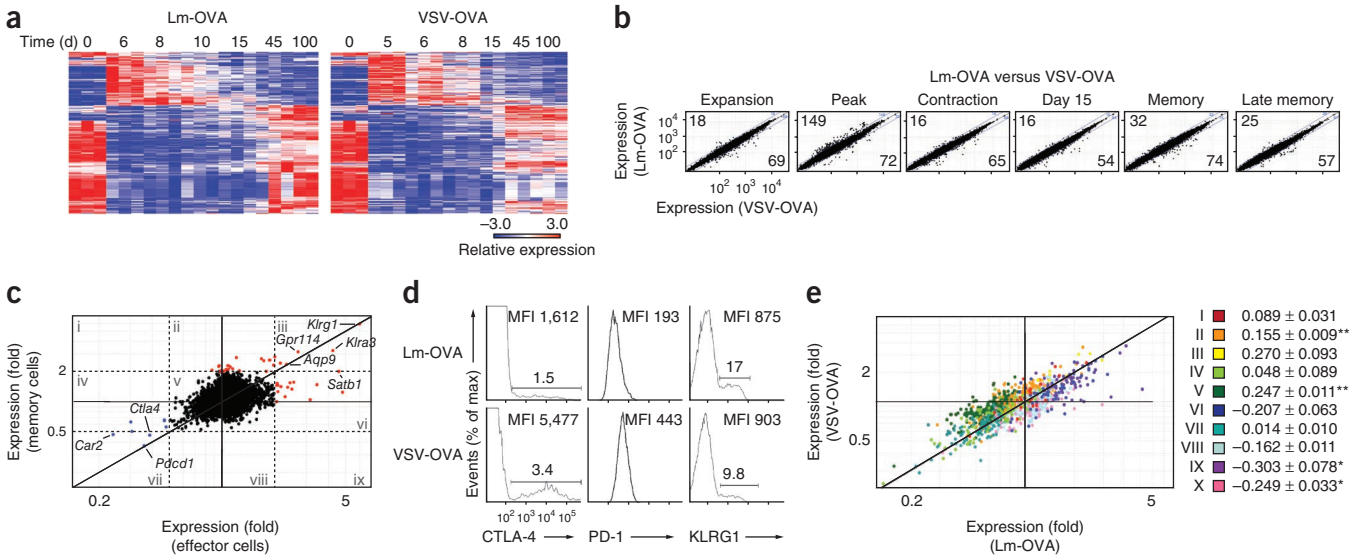

Figure 5 Regulation of genes associated with activation state is independent of infection. (**a**) Heat map of all genes upregulated or downregulated more than twofold in pooled effector cells relative to their expression in pooled memory cells during infection with Lm-OVA (LM) or VSV-OVA (VSV) at matching effector or memory time points (above plots). (**b**) Direct comparison of expression at each time point after infection with Lm-OVA or VSV-OVA; numbers in top left and bottom right corners indicate number of genes with difference in expression of over twofold (blue lines as in **Fig. 4a**). (**c**) Change in gene expression after infection with Lm-OVA versus VSV-OVA at pooled effector time points (horizontal axis) versus that at pooled memory time points (vertical axis); red, genes upregulated after infection with Lm-OVA; blue, genes upregulated after infection with VSV-OVA; labels indicate infection-specific genes of interest. (**d**) Flow cytometry of OT-I $CD8^+$ cells at day 6 of Lm-OVA infection or day 5 of VSV-OVA infection; numbers at top indicate median fluorescent intensity (MFI); numbers above bracketed lines indicate percent $CTLA\text{-}4^+$ cells (left) or $KLRG1^+$ cells (right) in gated populations. (**e**) Comparison of gene expression by pooled effector cells versus pooled memory cells after infection with Lm-OVA (horizontal axis) versus that comparison after infection with VSV-OVA (presented as in **Fig. 4b**). $^*P < 0.001$ and $^{**}P < 0.00001$ (*t*-test). Data are from three independent experiments with three mice (**a**–**c**,**e**) or four mice (**d**) per group.

or functional pathways conserved in activated $CD8^+$ T cells and other lineages (**Fig. 6a**). We defined 'enrichment' as the fraction of genes with a change in expression of over onefold. In confirmation of the validity of this approach, comparisons of germinal center and marginal zone B cells with follicular B cells showed very little correlation with any memory or effector-like clusters, whereas genes in clusters II and III (mostly encoding molecules involved in division and proliferation) had a significant bias for presence in germinal center B cells, an activated population. Conversely, we found strong correlations in certain subsets of cells known to have 'memory-like' traits, notably NKT cells and γδ T cells. NKT cells and $CD8^+$ memory T cells share a dependence on IL-15 for survival and homeostasis, rapid production of cytokines such as interferon-γ, cytolytic ability, expression of activation markers such as CD44, and the ability to rapidly respond to their cognate antigen. Thus, we might have expected all NKT cells to demonstrate a strong bias with our memory-specific

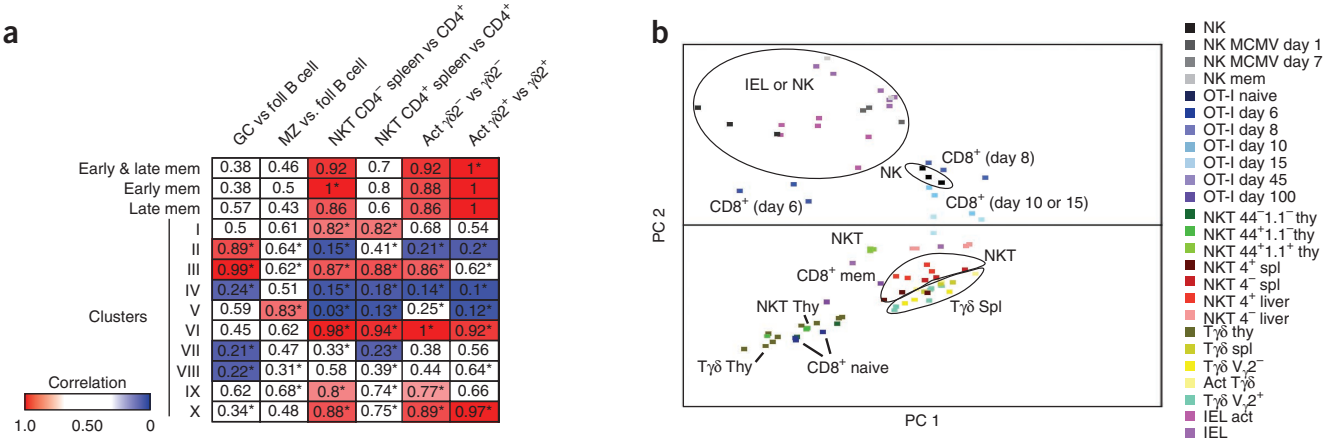

Figure 6 Genes induced in $CD8^+$ memory T cells correlate with gene expression by NKT cells and activated γδ T cells. (**a**) Heat map of the frequency of enrichment for $CD8^+$ T cell gene clusters (**Fig. 1c**) or memory-specific genes (**Fig. 1d**) in populations of B cells, NKT cells and γδ T cells. Red and blue (key) indicate cluster comparisons with the highest and lowest frequency of correlation (25%): red, higher frequency (>0.75); blue, lower frequency (<0.25). GC, germinal center; foll, follicular; MZ, marginal zone; act, activated; $\gamma\delta 2^+$, $V_\gamma 2^+$ γδ T cell; $\gamma\delta 2^-$, $V\gamma 2^-$ γδ T cell; mem, memory. $^*P < 0.05$ (χ^2 test). (**b**) Principle-component analysis of various cells (labels in plot and key) for genes defined in **Figure 1a**. MCMV, mouse cytomegalovirus; thy, thymus; spl, spleen; Tγδ, γδ T cell; IEL, intraepithelial lymphocyte. Data are pooled from three independent experiments with at least three mice per group.

gene sets generated above (**Fig. 1d**). However, the only population that showed significant bias toward expression of the 'memory specific' genes was splenic CD4$^-$ NKT cells, compared with resting CD4$^+$ T cells (**Fig. 6a**). This supported the idea that NKT cells bridge the gap between innate and adaptive immune responses. In contrast to other comparisons, which showed bias in only a few clusters, activated V$_\gamma$2$^+$ and V$_\gamma$2$^-$ γδ T cells showed highly significant bias for early and late memory gene sets, compared with resting γδ T cells.

To address those similarities further, we used principal-component analysis to visualize the variation among different innate subsets and memory T cells (**Fig. 6b**). We found that NKT cells mapped near memory T cells as well as γδ T cells, whereas NK cells, intraepithelial lymphocytes and effector CD8$^+$ T cells mapped together. Notably, the 'memory' NK cell population did not group with the CD8$^+$ memory populations in particular, which indicated that antigen-experienced NK cells were more similar to NK cell and CD8$^+$ effector T cell populations than to any of the memory populations analyzed. Together these data suggested that NKT cells and γδ T cells may share aspects of their transcriptional profile, as well as functional characteristics, with CD8$^+$ memory cells, whereas the gene-expression signature of CD8$^+$ effector T cells may be more similar to that of innate effector cells, including NK cells and intraepithelial lymphocytes.

DISCUSSION

Through the use of high-resolution microarray analyses, we sought to better understand the complexities of gene-expression changes during the course of infection, covering a range of CD8$^+$ T cell–activation states from early after activation to late memory. Using this data set, we identified clusters of genes with similar expression patterns, which allowed us to visualize core transcriptional changes during the immune response. By comparing the response of CD8$^+$ T cells to model antigens from bacterial and viral infections, we concluded that the transcriptional program governing effector and memory CD8$^+$ T cell differentiation is not necessarily tailored for viral versus bacterial pathogens, despite substantially different infection contexts. Furthermore, we found that monoclonal populations of CD8$^+$ T cells with transgenic expression of the TCR underwent differentiation events very similar to those of their endogenous polyclonal counterparts, which provided previously unavailable confirmation of the biological relevance of transgenic experimental models widely used in immunology. Together these data provide valuable insight into the transcriptional mechanisms of T cell activation and identify putative regulators of CD8$^+$ T cell responses, which offers a resource to the community.

The ten clusters in our analysis allowed us to correlate changes in gene expression with progressive stages of T cell activation and to identify, through evidence of coordinated regulation, previously unknown biological processes that operate during each stage. These clusters fit the present knowledge of gene expression and describe several known biological pathways in activated CD8$^+$ T cells but, notably, we identified many additional genes with characteristic expression kinetics during infection. One unexpected result was the prevalence of genes with strong neuronal association in cluster IV and memory-specific gene sets (*Nsg2*, *Cnr2*, *Cnrip1* and *Prss12*). Some of those genes, such as *Cnr2*, encode molecules with immunosuppressive effects in macrophages[32] and might have a role in maintaining homeostasis in naive and memory T cells. Similarly, members of the Schlafen 5 subfamily curb proliferation when expressed in T cells[33]. Many members of the S1P receptor family were also expressed, in addition to the proinflammatory molecule IL-12Rβ and the prosurvival chemokine receptor CX3CR1. The identification of IL-12Rβ was not unexpected, as IL-12 is known to drive CD8$^+$ T cells toward a terminally differentiated effector phenotype by inducing the transcription factor T-bet[19]; it is likely other receptor-ligand pairs identified in our analyses have similarly important roles in differentiation and memory formation.

Our analyses allowed a broad, unbiased look at gene-expression and regulatory networks involved in T cell activation. For example, consistent with published work, we identified the products of *Id2*, *Prdm1*, *Stat4* and *Tbx21* as potential regulators of cluster IV, which is one of the clusters mostly closely associated with terminally differentiated effector cells[34]. Our data identified RORα (clusters I, VI and X) as an additional potential regulator of CD8$^+$ effector cells, which is notable, as RORα expression is upregulated after antigen exposure, particularly at the peak of infection, and is important for the STAT3-dependant differentiation of CD4$^+$ cells of the T$_H$17 subset of helper T cells[35]. Notably, we identified the E proteins E2A (*Tcf3*; also known as *Tcfe2a*) and E2-2 (*Tcf4*) as potential repressors of clusters IV and VIII, which include genes expressed in naive and late effector-memory populations. Conversely, we identified Id2, ZEB1 and ZEB2, which all may inhibit later E-protein activity, as predicted activators of clusters I, VI, VIII, IX and X. By parsing genes expressed during CD8$^+$ T cell activation into clusters of common kinetic expression, we found many regulators potentially used to activate and/or repress multiple clusters. For example, we identified T-bet as an activator of clusters I, VII, VIII, IX and X but a repressor of cluster IV, which suggests its activity may serve not only to promote effector and effector-memory differentiation programs but also to repress naive and late-memory gene-expression signatures. Thus, we believe this strategy for identifying potential regulators of transcriptional signatures holds promise and will facilitate the elucidation of complex transcriptional networks that control the differentiation of effector and memory T cells at various points in the immune response. The results of our study have established a comprehensive transcriptional view of CD8$^+$ T cell activation, identifying new pathways and genes to be investigated in the context of CD8$^+$ immunity. The data set of the ImmGen Project and the identification and establishment of canonical gene clusters associated with different stages of CD8$^+$ T cell activation and differentiation provides a platform for future studies.

METHODS

Methods and any associated references are available in the online version of the paper.

Accession codes. GEO: microarray data, GSE15907.

Note: Supplementary information is available in the online version of the paper.

ACKNOWLEDGMENTS

We thank eBioscience, Affymetrix and Expression Analysis for support of the ImmGen Project. Supported by the US National Institutes of Health (AI072117 and AI067545 to A.W.G.; T32 AI060536 to J.A.B.; PN2 EY016586 to D.A.B. and M.L.D.; P30 CA016087 for cell sorting; and R24 AI072073 (National Institute of Allergy and Infectious Diseases) to the ImmGen Consortium), the Pew Scholars program (A.W.G.) and the Cancer Research Institute (A.W.G. and V.M.).

AUTHOR CONTRIBUTIONS

J.A.B. did experiments, designed studies, analyzed data and wrote the manuscript; J.K. sorted cell subsets and analyzed data; A.D. analyzed data and edited the manuscript; D.A.B., V.M. and M.L.D. designed and did early infection experiments, analyzed data and contributed to writing the manuscript; E.Y. sorted cell subsets; and A.W.G. designed studies, analyzed data and wrote the manuscript.

COMPETING FINANCIAL INTERESTS

The authors declare no competing financial interests.

1. Heng, T.S. & Painter, M.W. The Immunological Genome Project: networks of gene expression in immune cells. *Nat. Immunol.* **9**, 1091–1094 (2008).
2. Haining, W.N. *et al.* Identification of an evolutionarily conserved transcriptional signature of CD8 memory differentiation that is shared by T and B cells. *J. Immunol.* **181**, 1859–1868 (2008).
3. Kaech, S.M., Hemby, S., Kersh, E. & Ahmed, R. Molecular and functional profiling of memory CD8 T cell differentiation. *Cell* **111**, 837–851 (2002).
4. Sarkar, S. *et al.* Functional and genomic profiling of effector CD8 T cell subsets with distinct memory fates. *J. Exp. Med.* **205**, 625–640 (2008).
5. Wirth, T.C. *et al.* Repetitive antigen stimulation induces stepwise transcriptome diversification but preserves a core signature of memory CD8$^+$ T cell differentiation. *Immunity* **33**, 128–140 (2010).
6. Kaech, S.M. & Ahmed, R. Memory CD8$^+$ T cell differentiation: initial antigen encounter triggers a developmental program in naive cells. *Nat. Immunol.* **2**, 415–422 (2001).
7. Busch, D.H., Kerksiek, K.M. & Pamer, E.G. Differing roles of inflammation and antigen in T cell proliferation and memory generation. *J. Immunol.* **164**, 4063–4070 (2000).
8. Badovinac, V.P., Haring, J.S. & Harty, J.T. Initial T cell receptor transgenic cell precursor frequency dictates critical aspects of the CD8$^+$ T cell response to infection. *Immunity* **26**, 827–841 (2007).
9. Haluszczak, C. *et al.* The antigen-specific CD8$^+$ T cell repertoire in unimmunized mice includes memory phenotype cells bearing markers of homeostatic expansion. *J. Exp. Med.* **206**, 435–448 (2009).
10. Yamada, T., Park, C.S., Mamonkin, M. & Lacorazza, H.D. Transcription factor ELF4 controls the proliferation and homing of CD8$^+$ T cells via the Kruppel-like factors KLF4 and KLF2. *Nat. Immunol.* **10**, 618–626 (2009).
11. Beuneu, H. *et al.* Visualizing the functional diversification of CD8$^+$ T cell responses in lymph nodes. *Immunity* **33**, 412–423 (2010).
12. Grayson, J.M., Zajac, A.J., Altman, J.D. & Ahmed, R. Cutting edge: increased expression of Bcl-2 in antigen-specific memory CD8$^+$ T cells. *J. Immunol.* **164**, 3950–3954 (2000).
13. Gründemann, C. *et al.* Cutting edge: identification of E-cadherin as a ligand for the murine killer cell lectin-like receptor G1. *J. Immunol.* **176**, 1311–1315 (2006).
14. Dietz, S.B., Whitaker-Menezes, D. & Lessin, S.R. The role of αEβ7 integrin (CD103) and E-cadherin in epidermotropism in cutaneous T-cell lymphoma. *J. Cutan. Pathol.* **23**, 312–318 (1996).
15. Pearce, E.L. *et al.* Enhancing CD8 T-cell memory by modulating fatty acid metabolism. *Nature* **460**, 103–107 (2009).
16. Araki, K. *et al.* mTOR regulates memory CD8 T-cell differentiation. *Nature* **460**, 108–112 (2009).
17. van der Windt, G.J. *et al.* Mitochondrial respiratory capacity is a critical regulator of CD8$^+$ T cell memory development. *Immunity* **36**, 68–78 (2012).
18. Gautier, E.L. *et al.* Gene-expression profiles and transcriptional regulatory pathways that underlie the identity and diversity of mouse tissue macrophages. *Nat. Immunol.* **13**, 1118–1128 (2012).
19. Joshi, N.S. *et al.* Inflammation directs memory precursor and short-lived effector CD8$^+$ T cell fates via the graded expression of T-bet transcription factor. *Immunity* **27**, 281–295 (2007).
20. Rutishauser, R.L. *et al.* Transcriptional repressor Blimp-1 promotes CD8$^+$ T cell terminal differentiation and represses the acquisition of central memory T cell properties. *Immunity* **31**, 296–308 (2009).
21. Kaech, S.M. *et al.* Selective expression of the interleukin 7 receptor identifies effector CD8 T cells that give rise to long-lived memory cells. *Nat. Immunol.* **4**, 1191–1198 (2003).
22. Schluns, K.S., Kieper, W.C., Jameson, S.C. & Lefrancois, L. Interleukin-7 mediates the homeostasis of naive and memory CD8 T cells *in vivo*. *Nat. Immunol.* **1**, 426–432 (2000).
23. Huster, K.M. *et al.* Selective expression of IL-7 receptor on memory T cells identifies early CD40L-dependent generation of distinct CD8$^+$ memory T cell subsets. *Proc. Natl. Acad. Sci. USA* **101**, 5610–5615 (2004).
24. Yang, C.Y. *et al.* The transcriptional regulators Id2 and Id3 control the formation of distinct memory CD8$^+$ T cell subsets. *Nat. Immunol.* **12**, 1221–1229 (2011).
25. Cannarile, M.A. *et al.* Transcriptional regulator Id2 mediates CD8$^+$ T cell immunity. *Nat. Immunol.* **7**, 1317–1325 (2006).
26. D'Cruz, L.M., Lind, K.C., Wu, B.B., Fujimoto, J.K. & Goldrath, A.W. Loss of E protein transcription factors E2A and HEB delays memory-precursor formation during the CD8$^+$ T-cell immune response. *Eur. J. Immunol.* **8**, 2031–2041 (2012).
27. Harty, J.T. & Badovinac, V.P. Shaping and reshaping CD8$^+$ T-cell memory. *Nat. Rev. Immunol.* **8**, 107–119 (2008).
28. Obar, J.J., Khanna, K.M. & Lefrancois, L. Endogenous naive CD8$^+$ T cell precursor frequency regulates primary and memory responses to infection. *Immunity* **28**, 859–869 (2008).
29. Obar, J.J. *et al.* Pathogen-induced inflammatory environment controls effector and memory CD8$^+$ T cell differentiation. *J. Immunol.* **187**, 4967–4978 (2011).
30. Marzo, A.L. *et al.* Initial T cell frequency dictates memory CD8$^+$ T cell lineage commitment. *Nat. Immunol.* **6**, 793–799 (2005).
31. Agarwal, P. *et al.* Gene regulation and chromatin remodeling by IL-12 and type I IFN in programming for CD8 T cell effector function and memory. *J. Immunol.* **183**, 1695–1704 (2009).
32. Sacerdote, P., Massi, P., Panerai, A.E. & Parolaro, D. *In vivo* and *in vitro* treatment with the synthetic cannabinoid CP55, 940 decreases the *in vitro* migration of macrophages in the rat: involvement of both CB1 and CB2 receptors. *J. Neuroimmunol.* **109**, 155–163 (2000).
33. Geserick, P., Kaiser, F., Klemm, U., Kaufmann, S.H. & Zerrahn, J. Modulation of T cell development and activation by novel members of the Schlafen (slfn) gene family harbouring an RNA helicase-like motif. *Int. Immunol.* **16**, 1535–1548 (2004).
34. Kallies, A. Distinct regulation of effector and memory T-cell differentiation. *Immunol. Cell Biol.* **86**, 325–332 (2008).
35. Sundrud, M.S. & Rao, A. Regulation of T helper 17 differentiation by orphan nuclear receptors: it's not just RORγt anymore. *Immunity* **28**, 5–7 (2008).

ImmGen Project Consortium:

Paul Monach[4], Susan A Shinton[5], Richard R Hardy[5], Radu Jianu[6], David Koller[6], Jim Collins[7], Roi Gazit[8], Brian S Garrison[8], Derrick J Rossi[8], Kavitha Narayan[9], Katelyn Sylvia[9], Joonsoo Kang[9], Anne Fletcher[10], Kutlu Elpek[10], Angelique Bellemare-Pelletier[10], Deepali Malhotra[10], Shannon Turley[10], J Adam Best[1], Jamie Knell[1], Ananda W Goldrath[1], Vladimir Jojic[11], Daphne Koller[11], Tal Shay[12], Aviv Regev[12], Nadia Cohen[13], Patrick Brennan[13], Michael Brenner[13], Taras Kreslavsky[13], Natalie A Bezman[14], Joseph C Sun[14], Charlie C Kim[14], Lewis L Lanier[14], Jennifer Miller[15], Brian Brown[15], Miriam Merad[15], Emmanuel L Gautier[15,16], Claudia Jakubzick[15], Gwendalyn J Randolph[15,16], Francis Kim[17], Tata Nageswara Rao[17], Amy Wagers[17], Tracy Heng[18], Michio Painter[18], Jeffrey Ericson[18], Scott Davis[18], Ayla Ergun[18], Michael Mingueneau[18], Diane Mathis[18] & Christophe Benoist[18]

[4]Department of Medicine, Boston University, Boston, Massachusetts, USA. [5]Fox Chase Cancer Center, Philadelphia, Pennsylvania, USA. [6]Computer Science Department, Brown University, Providence, Rhode Island, USA. [7]Department of Biomedical Engineering, Howard Hughes Medical Institute, Boston University, Boston, Massachusetts, USA. [8]Immune Diseases Institute, Children's Hospital, Boston, Massachusetts, USA. [9]Department of Pathology, University of Massachusetts Medical School, Worcester, Massachusetts, USA. [10]Dana-Farber Cancer Institute and Harvard Medical School, Boston, Massachusetts, USA. [11]Computer Science Department, Stanford University, Stanford, California, USA. [12]Broad Institute, Cambridge, Massachusetts, USA. [13]Division of Rheumatology, Immunology and Allergy, Brigham and Women's Hospital, Boston, Massachusetts, USA. [14]Department of Microbiology & Immunology, University of California San Francisco, San Francisco, California, USA. [15]Icahn Medical Institute, Mount Sinai Hospital, New York, New York, USA. [16]Department of Pathology & Immunology, Washington University, St. Louis, Missouri, USA. [17]Joslin Diabetes Center, Boston, Massachusetts, USA. [18]Division of Immunology, Department of Microbiology & Immunobiology, Harvard Medical School, Boston, Massachusetts, USA.

ONLINE METHODS

Mice. Male C57BL/6J mice (Jackson Laboratories) were housed in specific pathogen–free conditions for 7–10 d before experimental use beginning at 6 weeks. CD45.1$^+$ OT-I mice deficient in recombination-activating gene 1 were bred and housed in specific pathogen–free conditions in accordance with the Institutional Animal Care and Use Guidelines of the University of California, San Diego.

Cell transfer and infection. For days 5–100 after infection, 5×10^3 CD45.1$^+$ OT-I cells were transferred into C57BL/6J recipient mice. Then, 1 d after T cell transfer, mice were infected with either 5×10^3 colony-forming units of Lm-OVA or 5×10^3 plaque-forming units of VSV-OVA. As OVA-specific T cells respond faster to VSV-OVA than to Lm-OVA, effector cells were collected on days 5, 6 and 8 of infection. For evaluation of the endogenous polyclonal T cell response, C57BL/6J mice were infected with 5×10^3 colony-forming units Lm-OVA or 1×10^5 plaque-forming units VSV. To obtain cells 12, 24 and 48 h after activation, 1×10^6 CD45.2$^+$ OT-I cells were transferred into CD45.1$^+$ C57BL/6J recipients. To obtain naive OT-I cells, 5×10^6 CD45.1$^+$ OT-I cells were injected into C57BL/6J mice and were purified from mice 2 d after transfer.

Cell sorting and flow cytometry. Cells were purified and analyzed according to the sorting protocol on the ImmGen Project website (http://www.immgen.org/Protocols/ImmGen Cell prep and sorting SOP.pdf). Flow cytometry of CD8$^+$ T cells from single-cell splenocyte suspensions to assess phenotype used the following antibodies (all from eBioscience): antibody to CD8 (anti-CD8; 53-6.7), anti-CD27 (LG-7F9), anti-CD44 (IM7), anti-CD45.1 (A20-1.7), anti- CD45.2 (104), anti-CD62L (MEL-14), anti-CD122 (TM-b1), anti-CD127 (A7R34) and anti-KLRG1 (2F1). Antigen-specific CD8$^+$ T cells were identified with a tetramer of H-2K^b and OVA peptide (sequence, SIINFEKL; Beckman Coulter). Antibodies were conjugated to fluorescein isothiocyanate, phycoerythrin, allophycocyanin or Alexa Fluor 780. Samples were collected on a FACSCalibur or FACSAria (BD Biosciences) and data were analyzed with FlowJo software (TreeStar).

Sample preparation for microarray analysis. RNA obtained from CD8$^+$CD45.1$^+$ cells (pooled from three mice) at various time points during infection with Lm-OVA or VSV-OVA was prepared in TRIzol reagent. RNA was amplified and hybridized to the Affymetrix Mouse Gene 1.0 ST Array. The GenePattern suite of genomic analysis software and the statistical environment R were used for microarray analysis. With the ImmGen profiling and quality-control pipelines, gene-expression profiles were generated on Affymetrix MoGene 1.0 ST arrays. All data analyzed passed quality-control criteria of the ImmGen Project with good replicate quality. The general ImmGen Project post-normalization threshold of 120 was taken to indicate positive expression (at 95% confidence), and probes were included in comparisons only if they were expressed by at least one cell type and with low variability in populations (coefficient of variation, <0.5).

Quantitative PCR. Donor cells were sorted as described above. RNA was extracted with TRIzol reagent (Invitrogen) and treated with DNAse (Ambion) and cDNA was generated with SuperScript III kit (Invitrogen). The abundance of mRNA was assessed by quantitative PCR with nonspecific product detection (SYBR Green; Stratagene) with primers that amplify in a linear relationship with primers for 'housekeeping' genes. Results were normalized to the expression of transcripts encoding GAPDH (glyceraldehyde phosphate dehydrogenase).

doi:10.1038/ni.2536